Automated Grading of Oral Squamous Cell Carcinoma into Multiple Classes Using Deep Learning Methods

1st Jelena Musulin
Department of Automation and Electronics
Faculty of Engineering - University of Rijeka
Rijeka, Croatia
jmusulin@riteh.hr

2nd Daniel Štifanić
Department of Automation and Electronics
Faculty of Engineering - University of Rijeka
Rijeka, Croatia
dstifanic@riteh.hr

3rd Ana Zulijani
Department of Oral Surgery
Clinical Hospital Center in Rijeka
Rijeka, Croatia
ana.zulijani@sz.uniri.hr

4th Sandi Baressi Šegota
Department of Automation and Electronics
Faculty of Engineering - University of Rijeka
Rijeka, Croatia
sbaressisegota@riteh.hr

5th Ivan Lorencin
Department of Automation and Electronics
Faculty of Engineering - University of Rijeka
Rijeka, Croatia
ilorencin@riteh.hr

6th Nikola Anđelić
Department of Automation and Electronics
Faculty of Engineering - University of Rijeka
Rijeka, Croatia
nandelic@riteh.hr

7th Zlatan Car
Department of Automation and Electronics
Faculty of Engineering - University of Rijeka
Rijeka, Croatia
car@riteh.hr

Abstract— **The diagnosis of oral squamous cell carcinoma is based on a histopathological examination, which is still the most reliable way of identifying oral cancer despite its high subjectivity. However, due to the heterogeneous structure and textures of oral cancer, as well as the presence of any inflammatory tissue reaction, histopathological classification can be difficult. For that reason, an automatic classification of histopathology images with the help of artificial intelligence-assisted technologies can not only improve objective diagnostic results for the clinician but also provide extensive texture analysis to get a correct diagnosis. In this paper various deep learning methods are compared in order to get an AI-based model for multiclass grading of OSCC with the highest AUC_{micro} and AUC_{macro} values.**

Keywords— artificial intelligence, deep learning methods, histopathology images, oral cancer

I. INTRODUCTION

Oral cancer (OC) is one of the most common malignant tumors in the world, and it has become an increasingly serious public health issue in developing and low-to-middle-income countries [1]. According to the GLOBOCAN database, there were an estimated 377 713 new cases diagnosed in 2020, with 177 757 deaths [2]. Despite advances in diagnostic and therapeutic approaches for OC patients, mortality and morbidity rates remain high, with no progress in the last 50 years, owing largely to late-stage diagnosis when tumor metastasis has occurred [3]. The most important risk factors for OC are the use of tobacco or betel quid and the regular drinking of alcoholic beverages, where more than 90% of cancers that occur in the cavity are squamous cell carcinoma

[4]. Surgical resection with or without adjuvant radiation is the most common procedure for oral squamous cell carcinoma (OSCC), which has a direct impact on patient living standards. The quality of life (QoL) of these patients is also related to the stage of the disease at the diagnosis, that is, on the extent of the surgical treatment which can impact oral dysfunction (presence of a feeding tube, speech and swallowing problems), social functioning and distress/anxiety [5]. Conventional oral examination (COE), clinical examination and histological evaluation following biopsy are currently the gold standard approaches for detecting OC. These procedures can detect cancer in the stage of established lesions with significant malignant changes [6]. The major difficulty in employing histological examination for tumor differentiation, and like prognostic factor, is the subjective component of the examination, i.e., inter-and intra-observer variability [7]. Moreover, as mentioned earlier, OC is more common in low-to-middle-income countries, where the number of oral cancer specialists is limited and patients in rural locations have even less access to proper diagnosis and treatment. As a result, with the rise of healthcare standards around the world, an overhaul of pathology is required, involving more rapid and precise diagnosis [8].

Nowadays, numerous Artificial Intelligence (AI) algorithms play important role in histopathology image analysis [9-11] as well as other various fields of medicine and science [12, 13]. Zhou et al. used Artificial Neural Network in order to improve the objectivity and accuracy of the breast histopathological analysis, while Tolkach et al. developed deep learning models for the detection of prostate cancer tissue based on histopathology images [14, 15]. Both papers

showed great results in terms of medical image analysis. Ai et al. in their paper demonstrated methods such as preprocessing, feature extraction, segmentation, and classification based on AI. Their results prove that there are many novel techniques that can be applied to gastric cancer histopathology analysis [16]. Musulin et al. proposed AI-system for automatic multiclass grading of OSCC and segmentation of the epithelial and stromal tissue from histopathological images. The proposed system based on preprocessing methods and deep Convolutional Neural Networks (CNN) achieved satisfactory results [17].

This paper is focused on the one segment – multiclass grading of OSCC using additional five deep learning models and it is an extension of aforementioned research [17]. Since every problem is different and challenging on its own way, it is necessary to apply various deep learning models on the problem from the field of interest and investigate obtained performances in order to bring quality conclusions. This way, results that are directly comparable with previous research will be obtained.

The main contributions are as follows;

• extension of previous work [17]; Investigating outcome of various deep learning models in terms of multiclass classification performances,

• by utilizing AI algorithms, histopathology tasks can be automated with high classification performance of models in order to improve the objectivity and reproducibility, respectively reducing inter-and intra-observer variability,

• furthermore, it could assist the specialist in terms of reducing the load of manual inspections as well as making fast decisions with higher precision.

II. MATERIALS AND METHODS

The Figure 1 shows the block diagram representation of the proposed methodology, and it can be described as follow; cases of OSCC that had been histopathologically reported will be retrieved from Clinical Hospital Center in Rijeka and classified by two unbiased pathologists. Then, original data will be augmented and used as an input variable to perform multiclass classification using AI models. Furthermore, the obtained results will be compared after the evaluation of models performance in order to select the best performing one.
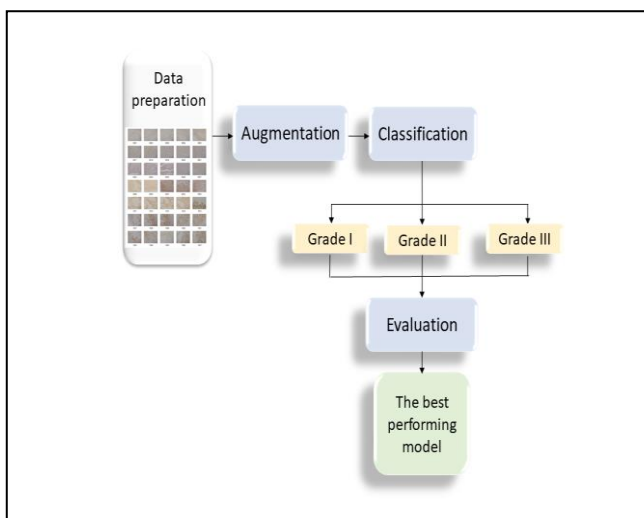

Fig. 1. Overall workflow of the paper

2.1 Dataset Description

The dataset used in this paper is collected from the archives of the Clinical Department of Pathology and Cytology at the Clinical Hospital Center in Rijeka, more specifically by taking the formalin-fixed, paraffin-embedded oral mucosa tissue blocks of histopathologically reported cases. It consists of 322 histopathological images with 768 x 768-pixel size which are divided into three classes: grade I (well-differentiated), grade II (moderately differentiated) and grade III (poorly differentiated) as shown in Figure 2. Full description of the data curation procedure is described in [17].
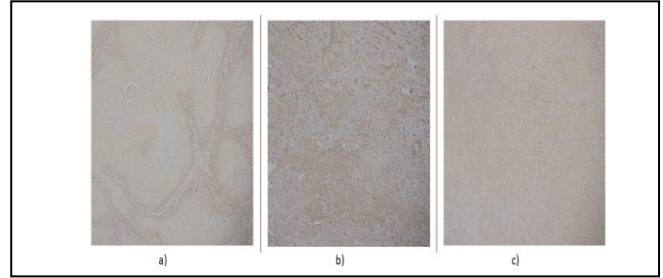

Fig. 2. Histopathology images of OSCC with magnification x10 where is: a) is grade I, b) grade II and c) grade III.

In order to obtain good performance and avoid overfitting, deep learning models rely substantially on a huge number of samples. Since areas such as medical image analysis rarely have access to a large number of samples, it is required to use augmentation techniques to significantly improve the amount and quality of the data. Due to the aforementioned deep learning models demand and restricted availability of the data, horizontal flip, horizontal flip combined with 90 degrees anticlockwise rotation, vertical flip, vertical flip combined with 90 degrees anticlockwise rotation, 90 degrees anticlockwise rotation, 180 degrees anticlockwise rotation and 270 degrees anticlockwise rotation are the geometrical transformations used for the augmentation procedure. This procedure is utilized just for the development of training samples (additional 1799 images) while test samples are not augmented.

2.2 Deep Learning Models

To estimate the performance of AI-based models, stratified 5-fold cross-validation is utilized due to the high imbalance of OSCC classes. As a result, the representation of each class across each test fold is roughly the same. AI-based models used in this paper are as follows;

• InceptionV3 – Following InceptionV1 and InceptionV2, Szegedy et al. proposed the idea of InceptionV3. It is primarily concerned with using less computational power by modifying previous Inception architectures. Several techniques for optimizing the network that have been proposed in an InceptionV3 to loosen the constraints for easier model adaptation are factorized convolutions, regularization, dimension reduction, and parallelized computations [18].

• InceptionResNetv2 – Since the Inception architecture has been proven successful at relatively low computational cost Szegedy et al. introduce the InceptionResNetv2 that combines the Inception architecture with residual connections. Presented architecture improved recognition performance as well as improved training speed [19].

• DenseNet – Huang et al. demonstrated Dense Convolutional Network (DenseNet), a feed-forward network that connects each layer to every other layer. Such network has a number of appealing advantages, including the elimination of the vanishing-gradient problem, improved feature propagation, encourage feature reuse, and a significant reduction of number of parameters. DenseNets achieved significant results over many state-of-the-art methods while using less computatonal power to reach good performance [20].

• NASNet – Zoph et al. introduce Neural Architecture Search Network called NASNet where they propose to search an architectural building block on a small dataset and then transfer it to a larger dataset. In their research, they look for the best convolutional layer on the CIFAR-10 dataset. Then, apply it to the ImageNet dataset by stacking many copies of it, each with its own set of parameters, to create a convolutional architecture. Furthermore, they introduce ScheduledDropPath, a new regularization method that significantly enhances generalization in NASNet models [21].

• EfficientNet – In their paper, Tan and Lee propose a novel scaling method called EfficientNet. Such a method, to scale up CNNs in a more structured manner, employs a simple yet highly effective compound coefficient. According to the authors, EfficientNets by significantly improving model efficiency, could potentially serve as a new foundation for future computer vision tasks [22].

2.3 Evaluation Critera

In order to evaluate the classification performance of models, statistical measures such as micro and macro area under the curve (AUC) are used. AUC_{micro} and AUC_{macro} can be calculated by micro and macro averaging, respectively. In micro averaging of true positive rate (TPR), the number of valid classifications for each class is calculated and used as the numerator, while the total number of samples is used as the denominator. Moreover, the ratio of false classifications for each class to the total number of samples is calculated by the fallout or false positive rate (FPR) [23]. The following is a mathematical description of AUC micro averaging [17]:

$$TPRmicro = \frac{\sum_{i=1}^{k} TPi}{\sum_{i=1}^{k} TPi + \sum_{i=1}^{k} FNi} \qquad (1)$$

and

$$FPRmicro = \frac{\sum_{i=1}^{k} FPi}{\sum_{i=1}^{k} FPi + \sum_{i=1}^{k} TNi} \qquad (2)$$

where:

• TP – are true positives, or cases where the predicted and actual values are both positive.

• TN – are true negatives, or cases where the actual and predicted values are both negative.

• FN – are false negatives or cases in which a negative prediction is made but the actual value is positive.

• FP – are false positives that occur when the prediction is positive, but the actual value is negative [24].

Macro averaging for k classes computes the metrics for each class separately and then averages the results. TPR_{macro} and FPR_{macro} are used to calculate AUC_{macro} and can be expressed as [17]:

$$TPRmacro = \frac{\sum_{i=1}^{k} TPRi}{k} \qquad (3)$$

and

$$FPRmacro = \frac{\sum_{i=1}^{k} FPRi}{k}. \qquad (4)$$

By definition the Receiver Operator Characteristic (ROC) curve is a metric used for evaluation mainly in binary classification problems. It is considered as a probability curve which can be plotted with FPR on the x-axis, TPR on y-axis. In order to summarize the ROC curve, AUC measure is used which calculates the area underneath the ROC curve. To extend AUC to multiclass classification, it is necessary to conceptualize the problem as a binary classification problem, by using One vs. All technique, which means that one class is classified against all other classes. More precisely AUC_{micro} and AUC_{macro} are based on the calculation of TPR_{micro} as well as FPR_{micro}, and TPR_{macro} along with FPR_{macro}, respectively.

III. RESULTS AND DISCUSSION

This section demonstrates the AUC_{macro} and AUC_{micro} of deep learning models pre-trained on ImageNet. The experimental results were obtained with InceptionV3, InceptionResNetV2, DenseNet201, NASNet and EfficientNetB3 arhitectures.
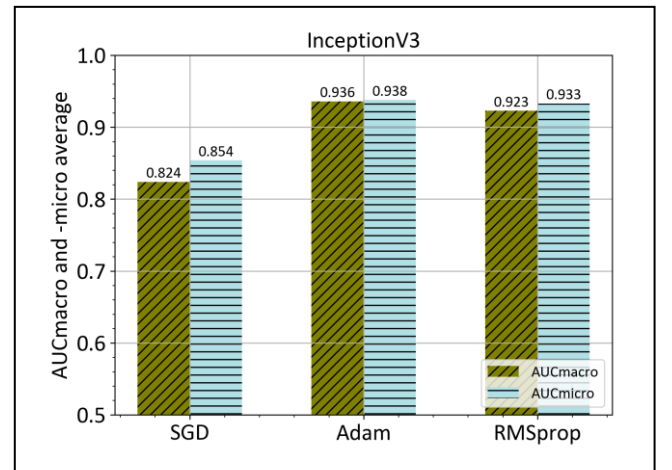

Fig. 3. AUC_{macro} and AUC_{micro} values of three different optimizers utilizing InceptionV3 architecture

In case of InceptionV3 the highest AUC_{macro} and AUC_{micro} values of 0.936 ($\pm\sigma$ = 0.051) and 0.938 ($\pm\sigma$ = 0.048) are achieved with Adam optimizer as shown in Figure 3. However, InceptionV3 in combination with stochastic gradient descent (SGD) optimizer achieves the lowest values.
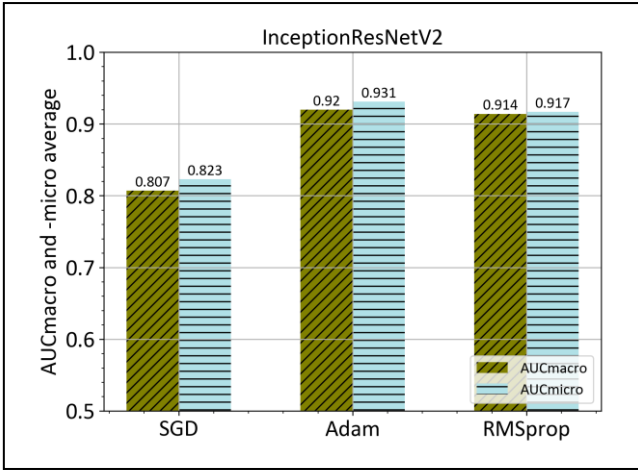
Fig. 4. AUC_{macro} and AUC_{micro} values of three different optimizers utilizing InceptionResNetV2 arhitecture

Same as the previous case, by using the Adam optimizer and InceptionResNetV2 architecture the highest AUC_{macro} of 0.920 ($\pm\sigma = 0.059$) and AUC_{micro} of 0.931 ($\pm\sigma = 0.0064$) are achieved as shown in Figure 4.
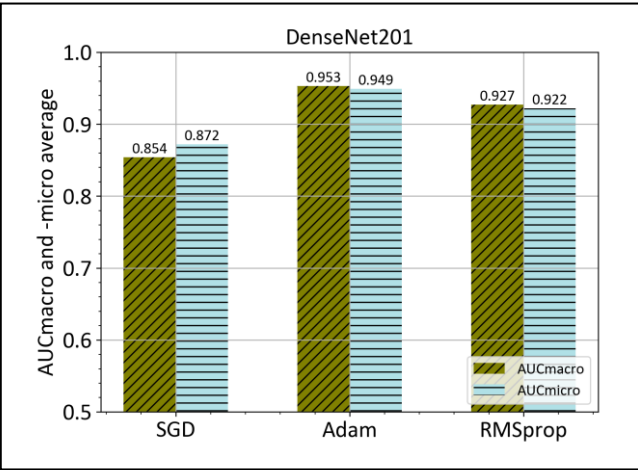

Fig. 5. AUC_{macro} and AUC_{micro} values of three different optimizers utilizing DenseNet201 arhitecture

Figure 5 shows that DenseNet201 architecture in combination with Adam optimizer achieves overall highest AUC_{macro} and AUC_{micro} values of 0.953 ($\pm\sigma = 0.043$) and 0.949 ($\pm\sigma = 0.041$), respectively. Moreover, the lowest values are achieved in combination with SGD optimizer, where AUC_{macro} is 0.854 ($\pm\sigma = 0.082$) and AUC_{micro} 0.872 ($\pm\sigma = 0.036$).

Figure 6 shows that Adam optimizer in combination with NASNet architecture achieves the highest AUC_{macro} value of 0.890 ($\pm\sigma = 0.054$) and AUC_{micro} value of 0.909 ($\pm\sigma = 0.043$). Unlike the previous cases, the lowest AUC_{macro} and AUC_{micro} values are achieved with RMSprop optimizer.
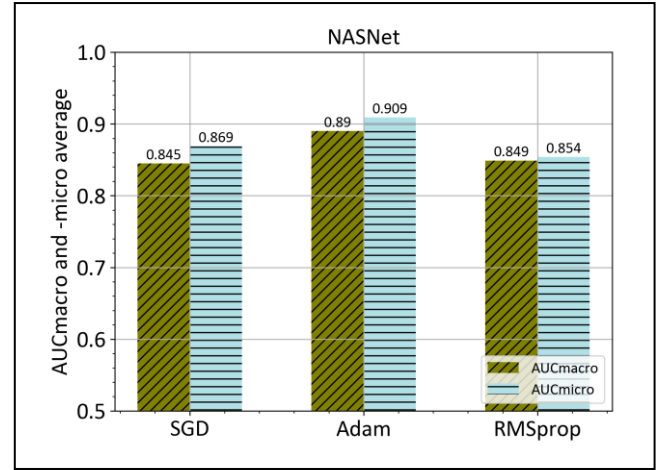

Fig. 6. AUC_{macro} and AUC_{micro} values of three different optimizers utilizing NASNet arhitecture
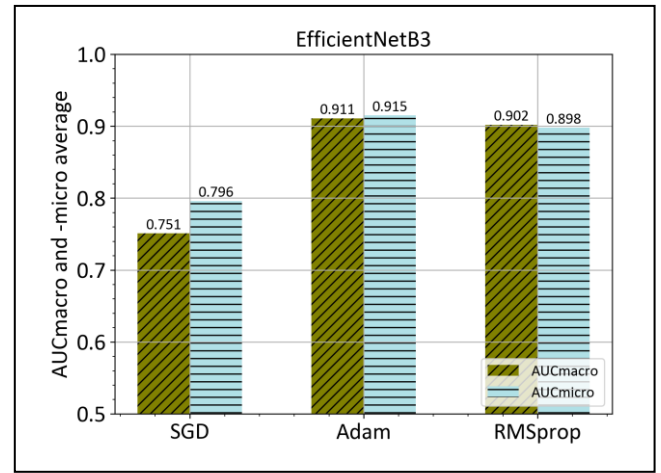

Fig. 7. AUC_{macro} and AUC_{micro} values of three different optimizers utilizing EfficientNetB3 arhitecture

The highest AUC_{macro} of 0.911 ($\pm\sigma = 0.148$) and AUC_{micro} of 0.915 ($\pm\sigma = 0.148$) obtained on pretrained EfficientNetB3 are shown in Figure 7.

Literature reveals that most of the researchers have applied deep Convolutional Neural Networks in their study for cancer classification based on histopathology images. Celik et al. used deep learning pre-trained models in order to detect invasive ductal carcinoma. The model with the best-balanced accuracy (91.57%) was DenseNet-161 while the model with the highest F-score (94.11%) was ResNet-50 [25]. Han et al. show another AI solution in a similar area of study. They propose a newly developed deep learning model called CSDCNN in order to perform automated breast cancer multi-classification. Based on the remarkable performance of the model (accuracy $\approx$ 93%) they proved that such an approach can be an efficient tool in clinical settings for breast cancer classification [26]. Shirazi et al. used deep survival convolutional network (DeepSurvNet) on histopathological brain cancer dataset to classify four classes of patients' survival rates. Results of 99% precision show that DeepSurvNet could help in the evaluation of patient treatment [27]. Sarkar et al. demonstrated modified DenseNet for classifying the colorectal histopathology images into nine classes. The achieved accuracy of 97.2% was better than most of the contemporary works in that domain [28]. Based on a literature study only two papers [8, 17] proposed a deep

learning model for the multiclass classification of oral squamous cell carcinoma using histopathological images. Das et al. perform their CNN model on image patches derived from whole slide biopsy. Presented model resulted in 97.5% accuracy [8]. On the other hand, Musulin et al. achieved the highest classification value of 0.963 AUCmacro and 0.966 AUCmicro by integrating Xception with preprocessing method based on stationary wavelet transform and proposed mapping function. However, Xception without preprocessing achieves AUCmacro and AUCmicro values of 0.929 and 0.942, respectively [17].

In this paper different Deep Learning Models without preprocessing are applied on the same problem as in [17] in order to investigate the influence on the overall outcome in terms of multiclass classification performance.

The overall best results are achieved when, at the top of the base DenseNet201 architecture, two additional layers were added. First added layer was global average pooling, while the second one was the fully connected layer i.e., the output layer. Since the main challenge of this study was multiclass grading of OSCC (grade I, grade II, and grade III), the last layer consisted of three neurons, by which, classification into three classes was enabled. Moreover, Softmax was used as the activation function. The model training process was divided into two stages; in the first stage, all the layers were frozen except the added layers, while in the second stage all base model layers were trainable except the last two added layers. The training process in the first stage was performed with a learning rate of 0.001, and a learning rate decay of 1e-6. Furthermore, in the second stage, the learning rate was set on a lower value of 0.0001 since these layers were already pretrained on ImageNet. Additionally, in the second stage, the learning rate decay remained the same with the value of 1e-6. The overall lowest values of standard deviation in the case where AUC_{macro} and AUC_{micro} were higher than 0.9 were achieved by utilizing DenseNet201 architecture with RMSprop as an optimizer with the standard deviation values of $\pm\sigma = 0.033$ and $\pm\sigma = 0.031$, respectively. Such values of standard deviation indicate high robustness of the model which, in a combination with high values of performance measure, has a great potential as an assistive tool in medical image analysis.

IV. Conclusion

This paper demonstrates the enormous potential of using AI-based algorithms to achieve an accurate prognosis of OSCC and increase people's chances of survival. For the multiclass classification problem authors compared various deep learning models with different configuration settings in order to achieve satisfactory classification performance. From obtained results, it can be concluded that the base DenseNet201 architecture with added two additional layers resulted in highest classification values of 0.953 AUC_{macro} and 0.949 AUC_{micro} with the lowest standard deviation of $\pm\sigma = 0.043$ and $\pm\sigma = 0.041$, respectively.

Since data availability was a limitation of this study, future work should use a dataset with more histopathology images to achieve a more robust model. Furthermore, this paper is the base study in histopathology image analysis where the main idea is to develop an automated prognostic system that might contribute to improving a patient's prognosis and survival rate along with modified treatment planning.

References

[1] H. Lin, H. Chen, L. Weng, J. Shao, and J. Lin, "Automatic detection of oral cancer in smartphone-based images using deep learning for early diagnosis," Journal of Biomedical Optics, vol. 26, no. 08, 2021.

[2] H. Sung, J. Ferlay, R. L. Siegel, M. Laversanne, I. Soerjomataram, A. Jemal, and F. Bray, "Global cancer STATISTICS 2020: GLOBOCAN estimates of incidence and MORTALITY worldwide for 36 cancers in 185 COUNTRIES," CA: A Cancer Journal for Clinicians, vol. 71, no. 3, pp. 209–249, 2021.

[3] J. Bagan, G. Sarrion, and Y. Jimenez, "Oral cancer: Clinical features," Oral Oncology, vol. 46, no. 6, pp. 414–417, 2010.

[4] L. Feller and J. Lemmer, "Oral squamous cell carcinoma: Epidemiology, clinical presentation and treatment," Journal of Cancer Therapy, vol. 03, no. 04, pp. 263–268, 2012.

[5] K. S. Ettinger, L. Ganry, and R. P. Fernandes, "Oral cavity cancer," Oral and Maxillofacial Surgery Clinics of North America, vol. 31, no. 1, pp. 13–29, 2019.

[6] S. Warnakulasuriya, J. Reibel, J. Bouquot, and E. Dabelsteen, "Oral epithelial dysplasia classification systems: Predictive value, utility, weaknesses and scope for improvement," *Journal of Oral Pathology & Medicine*, vol. 37, no. 3, pp. 127–133, 2008.

[7] C. S. Mehlum, S. R. Larsen, K. Kiss, A. M. Groentved, T. Kjaergaard, S. Möller, and C. Godballe, "Laryngeal precursor LESIONS: Interrater and intrarater reliability OF Histopathological assessment," *The Laryngoscope*, vol. 128, no. 10, pp. 2375–2379, 2018.

[8] N. Das, E. Hussain, and L. B. Mahanta, "Automated classification of cells into multiple classes in epithelial tissue of oral squamous cell carcinoma using transfer learning and convolutional neural network," *Neural Networks*, vol. 128, pp. 47–60, 2020.

[9] X. Shi, H. Su, F. Xing, Y. Liang, G. Qu, and L. Yang, "Graph temporal ensembling based semi-supervised convolutional neural network with noisy labels for histopathology image analysis," *Medical Image Analysis*, vol. 60, p. 101624, 2020.

[10] X. Zhou, C. Li, M. M. Rahaman, Y. Yao, S. Ai, C. Sun, Q. Wang, Y. Zhang, M. Li, X. Li, T. Jiang, D. Xue, S. Qi, and Y. Teng, "A comprehensive review for breast histopathology image analysis using classical and deep neural networks," *IEEE Access*, vol. 8, pp. 90931–90956, 2020.

[11] C. Li, H. Chen, X. Li, N. Xu, Z. Hu, D. Xue, S. Qi, H. Ma, L. Zhang, and H. Sun, "A review for cervical histopathology image analysis using machine vision approaches," *Artificial Intelligence Review*, vol. 53, no. 7, pp. 4821–4862, 2020.

[12] I. Lorencin, N. Anđelić, S. Baressi Šegota, J. Musulin, D. Štifanić, V. Mrzljak, J. Španjol, and Z. Car, "Edge detector-based hybrid artificial neural network models for urinary bladder cancer diagnosis," *Enabling AI Applications in Data Science*, pp. 225–245, 2020.

[13] D. Štifanić, J. Musulin, Z. Jurilj, S. Šegota, I. Lorencin, N. Anđelić, S. Vlahinić, T. Šušteršič, A. Blagojević, N. Filipović, and Z. Car, "Semantic segmentation of chest x-ray images based on the severity of COVID-19 infected patients," *EAI Endorsed Transactions on Bioengineering and Bioinformatics*, vol. 1, no. 3, p. 170287, 2021.

[14] X. Zhou, C. Li, M. M. Rahaman, Y. Yao, S. Ai, C. Sun, Q. Wang, Y. Zhang, M. Li, X. Li, T. Jiang, D. Xue, S. Qi, and Y. Teng, "A comprehensive review for breast histopathology image analysis using classical and deep neural networks," *IEEE Access*, vol. 8, pp. 90931–90956, 2020.

[15] Y. Tolkach, T. Dohmgörgen, M. Toma, and G. Kristiansen, "High-accuracy prostate cancer pathology using deep learning," *Nature Machine Intelligence*, vol. 2, no. 7, pp. 411–418, 2020.

[16] S. Ai, C. Li, X. Li, T. Jiang, M. Grzegorzek, C. Sun, M. M. Rahaman, J. Zhang, Y. Yao, and H. Li, "A state-of-the-art review for Gastric

Histopathology image Analysis approaches and future development," *BioMed Research International*, vol. 2021, pp. 1–19, 2021.

[17] J. Musulin, D. Štifanić, A. Zulijani, T. Ćabov, A. Dekanić, and Z. Car, "An enhanced HISTOPATHOLOGY Analysis: AN AI-Based system for MULTICLASS grading of Oral squamous cell carcinoma and SEGMENTING of epithelial And stromal tissue," *Cancers*, vol. 13, no. 8, p. 1784, 2021.

[18] C. Szegedy, V. Vanhoucke, S. Ioffe, J. Shlens, and Z. Wojna, "Rethinking the Inception architecture for computer vision," 2016 IEEE Conference on Computer Vision and Pattern Recognition (CVPR), 2016.

[19] C. Szegedy, S.Ioffe, V. Vanhoucke, and A.A. Alemi, " Inception-v4, inception-resnet and the impact of residual connections on learning," In Thirty-first AAAI conference on artificial intelligence, 2017.

[20] G. Huang, Z. Liu, L. Van Der Maaten, and K. Q. Weinberger, "Densely connected convolutional networks," 2017 IEEE Conference on Computer Vision and Pattern Recognition (CVPR), 2017.

[21] B. Zoph, V. Vasudevan, J. Shlens, and Q. V. Le, "Learning transferable architectures for scalable image recognition," 2018 IEEE/CVF Conference on Computer Vision and Pattern Recognition, 2018.

[22] M. Tan and Q. Le. ""Efficientnet: Rethinking model scaling for convolutional neural networks." International Conference on Machine Learning.," *2019 International Conference on Machine Learning, pp. 6105-6114, 2019.*

[23] A. Tharwat, "Classification assessment methods," *Applied Computing and Informatics*, vol. 17, no. 1, pp. 168–192, 2020.

[24] L. C. Leonard, "Web-Based behavioral modeling for Continuous user Authentication (CUA)," *Advances in Computers*, pp. 1–44, 2017.

[25] Y. Celik, M. Talo, O. Yildirim, M. Karabatak, and U. R. Acharya, "Automated invasive ductal carcinoma detection based using deep transfer learning with whole-slide images," Pattern Recognition Letters, vol. 133, pp. 232–239, 2020.

[26] Z. Han, B. Wei, Y. Zheng, Y. Yin, K. Li, and S. Li, "Breast cancer multi-classification from histopathological images with structured deep learning model," Scientific Reports, vol. 7, no. 1, 2017.

[27] A. Zadeh Shirazi, E. Fornaciari, N. S. Bagherian, L. M. Ebert, B. Koszyca, and G. A. Gomez, "DeepSurvNet: Deep survival convolutional network for Brain Cancer Survival Rate Classification based on histopathological images," Medical & Biological Engineering & Computing, vol. 58, no. 5, pp. 1031–1045, 2020.

[28] T. Sarkar, A. Hazra, and N. Das, "Classification of colorectal cancer histology images using image reconstruction and modified DenseNet," Communications in Computer and Information Science, pp. 259–271, 2021.